Chemistry & Biology, Vol. 11, 535–546, April, 2004, ©2004 Elsevier Science Ltd. All rights reserved. DOI 10.1016/j.chembiol.2004.03.012

Profiling Enzyme Activities In Vivo Using Click Chemistry Methods

Anna E. Speers and Benjamin F. Cravatt*
The Skaggs Institute for Chemical Biology
Departments of Chemistry and Cell Biology
The Scripps Research Institute
10550 North Torrey Pines Road
La Jolla, California 92037

Summary

Methods for profiling the activity of enzymes in vivo are needed to understand the role that these proteins and their endogenous regulators play in physiological and pathological processes. Recently, we introduced a tag-free strategy for activity-based protein profiling (ABPP) that utilizes the copper(I)-catalyzed azide-alkyne cycloaddition reaction ("click chemistry") to analyze the functional state of enzymes in living cells and organisms. Here, we report a detailed characterization of the reaction parameters that affect click chemistry-based ABPP and identify conditions that maximize the speed, sensitivity, and bioorthogonality of this approach. Using these optimized conditions, we compare the enzyme activity profiles of living and homogenized breast cancer cells, resulting in the identification of several enzymes that are labeled by activity-based probes in situ but not in vitro.

Introduction

The continuing success of genome sequencing efforts has laid the foundation for understanding the molecular basis of life in its many forms. However, this task involves not only the characterization of genes but the products of gene expression as well. As primary mediators of most physiological and pathological processes, proteins may be viewed as the next major challenge, especially considering the difficulties involved in developing and applying methods for the global analysis of proteins (proteomics) as compared to DNA or RNA molecules (genomics) [1]. For example, unlike oligonucleotides, proteins exhibit a diverse array of chemical and biochemical properties, are not amenable to molecular amplification, and do not possess predefined complementary binding partners. Despite the many technical challenges that accompany the analysis of proteins, the need for global strategies to characterize the expression and function of these biomolecules is clear, especially given the multitude of posttranscriptional and posttranslational processes that regulate the activity of proteins in cells and tissues [2].

Initial strategies for proteomics sought to collectively profile the expression levels of proteins using two-dimensional gel electrophoresis (2DE), staining, and mass spectrometry (MS) for protein separation, quantitation, and identification, respectively [3]. However, 2DE methods suffer from a lack of resolving power [4–6], which limits their ability to detect certain classes of proteins, including membrane-associated and low-abundance proteins. More advanced strategies for proteome analysis have subsequently been introduced, including isotope-coded affinity tagging (ICAT) [7], which enables the comparative analysis of protein expression levels by liquid chromatography-tandem MS (LC-MS/MS). LC-based strategies have overcome some of the resolution problems of 2DE, providing improved access to membrane-associated and low-abundance proteins [8]; however, these techniques, like 2DE, focus primarily on measuring variations in protein abundance and therefore provide only an indirect estimate of changes in protein activity.

In response to these limitations, activity-based protein profiling (ABPP) has been introduced as a complement to abundance-based genomic and proteomic techniques [9, 10]. ABPP utilizes active site-directed chemical probes to determine the functional state of enzymes in complex proteomes, distinguishing, for example, active enzymes from their inactive precursors (e.g., zymogens) [11] and/or inhibitor-bound forms [11–13]. ABPP probes consist of at least two elements: (1) a reactive group (RG) for binding to and covalently labeling the active sites of many members of an enzyme class (or classes) and (2) one or more reporter tags (e.g., biotin and/or a fluorophore) for the rapid detection and isolation of probe-labeled enzymes (Figure 1A). A binding group (BG) may also be used to promote probe interactions with particular enzyme active sites. To date, activity-based probes have been developed for over a dozen classes of enzymes, including serine hydrolases [11, 12], cysteine proteases [13–16], protein tyrosine phosphatases [17], and glycosidases [18], as well as multiple oxidoreductases [19, 20] (for review see [21]).

However, in pursuit of the ultimate goal of characterizing the function of all proteins in parallel and in the most physiologically relevant settings possible (i.e., in vivo), ABPP, like other proteomic approaches, is still in need of improvement. For example, until recently, ABPP experiments were conducted almost exclusively with cell and tissue homogenates rather than living cells and organisms. Because physical disruption of cells/tissues may alter the concentrations of endogenous protein activators/inhibitors, as well as their subcellular distributions, in vitro proteomic preparations can only approximate the functional state of proteins in a living cell or organism. A traditional limitation to applying ABPP probes in vivo has been the nature of their bulky reporter tags, which are typically quite large (700–1000 Da) and therefore limit probe uptake and distribution in cells and tissues. Thus, to accommodate in vivo profiling, a "tag-free" version of ABPP was introduced, whereby a reporter group could be attached to the activity-based probe following covalent labeling of enzyme targets [22] (Figure 1B). This conjugation step was accomplished by engineering into the probe and tag a pair of small, bioorthogonal coupling partners, the azide and alkyne, which can react via Huisgen's 1,3-dipolar cycloaddition

*Correspondence: cravatt@scripps.edu

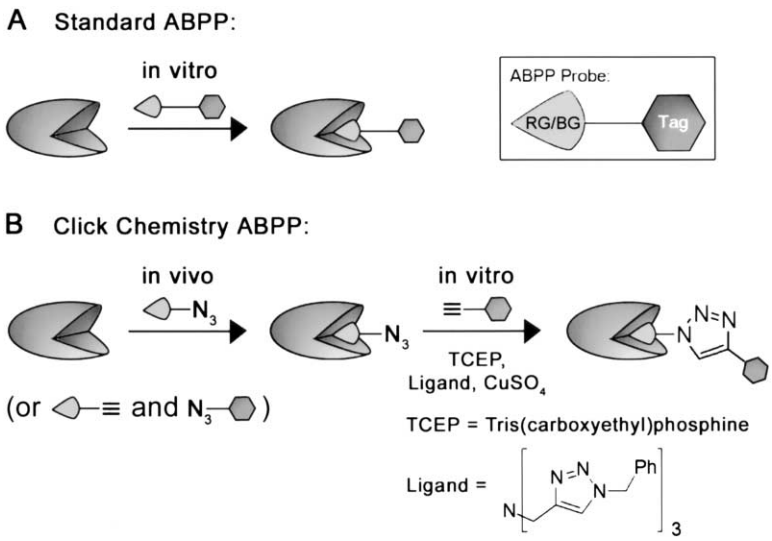

Figure 1. Comparison of Standard and Click Chemistry ABPP

ABPP probes consist of a reactive group (RG), binding group (BG), and tag (e.g., rhodamine and/or biotin). In contrast to standard ABPP, click chemistry ABPP allows for the profiling of living cells and organisms by treating these specimens with tag-free azide- or alkyne-modified probes, which are then conjugated in vitro to the complementary alkyne- or azide-modified tag under cycloaddition reaction conditions to visualize probe-labeled proteins.

to form a stable triazole product. This cycloaddition reaction is typically quite slow [23, 24], and it was not until the Sharpless [25] and Meldal [26] labs reported a Cu(I)-catalyzed stepwise analog of Huisgen's concerted triazole synthesis ("click chemistry" [23]) and Finn and colleagues demonstrated its general biocompatibility [27] that this reaction became potentially feasible for ABPP. (For review see [28].) Using the click chemistry (CC) methodology, we were able to label several enzymes with an azido-phenyl sulfonate ester activity-based probe, both in vivo and in cell/tissue homogenates, effect conjugation of an alkyne-tag via the cycloaddition reaction, and separate/visualize the probe-labeled proteins by gel electrophoresis and fluorescence scanning [22]. The general success of such a tag-free approach was further validated by the recent report by Ovaa et al. describing the in vivo profiling of the proteasome using the Staudinger ligation for probe-tag conjugation [29].

However, one drawback to CC-ABPP was noted in our previous report [22]—the methodology suffered from higher background labeling as compared to conventional ABPP. These background signals, which appeared to derive from low-level nonspecific labeling of abundant proteins in the proteome, obscured the detection of some low-abundance specific targets of azido activity-based probes, thus limiting the sensitivity of CC-ABPP. We now report the successful resolution of this problem, as well as an optimized cycloaddition reaction protocol for CC-ABPP, including methodologies for protein labeling, isolation, and identification. Using these optimized conditions, we have conducted a comparative analysis of the enzyme activity profiles of living and homogenized human breast cancer cells, resulting in the identification of several enzymes that were labeled by activity-based probes in situ but not in vitro.

Results

Testing the Effects of Probes, Tags, and Reaction Parameters on the Specific and Nonspecific Reactivity of Click Chemistry-ABPP

In our initial report of click chemistry (CC)-ABPP, an azide-modified phenyl sulfonate ester activity-based probe (PSN_3, **1**) and an alkyne-derivatized rhodamine reporter tag (Rh≡, **4**) (Figure 2) were used to profile enzyme activities in complex proteomes. This tag-free strategy for ABPP proved capable of profiling several enzyme activities both in vitro and in vivo; however, a direct comparison of CC- and standard ABPP revealed that the former method suffered from higher background (i.e., heat-insensitive, nonspecific) labeling with proteomes, which reduced its sensitivity and hindered the detection of specifically labeled low-abundance targets of the PSN_3 probe [22]. Here, we have systematically varied key reaction parameters of CC-ABPP to determine the basis for the elevated background reactivity. Interestingly, removal of the PSN_3 probe did not markedly affect the intensity of background labeling observed in either cell or tissue proteomes (Figure 3A, lanes 1 and 7), indicating that these signals corresponded to an SDS-stable (probably covalent) association between proteins and the Rh≡ reporter tag. Rh≡ background reactivity required $CuSO_4$ (Figure 3B, lane 4 versus 5) and further increased when the ligand and/or reducing agent tris(carboxyethyl)phosphine (TCEP) were also included in the reaction (Figure 3B, lanes 1–3). Although the chemical basis for protein labeling by Rh≡ remains unknown, an alkane analog of Rh≡ did not exhibit any reactivity with proteomes (data not shown), indicating that the alkyne is responsible for protein modification. Given these findings, we next tested whether switching the directionality of the cycloaddition reaction would circumvent the increased background labeling of CC-ABPP.

Two alkyne phenyl sulfonate ester probes (PS4≡, **2** and PS9≡, **3**) and a rhodamine-azide tag (RhN_3, **5**) were synthesized (Figure 2), and proteome reactions with these reagents were compared to those with the PSN_3/Rh≡ pair. The soluble fraction (cytosol) of homogenized tissue (mouse heart) or cell (human MDA-MB-435 cancer cell line) proteomes was incubated with probe (5 μM) for 1 hr, and then the complementary tag (50 μM) was added to reactions, followed by TCEP (1 mM), ligand (100 μM, see Figure 1B for structure), and $CuSO_4$ (1 mM). After 1 hr, reactions were analyzed by 1D-SDS-PAGE and in-gel fluorescence scanning. As shown in Figure

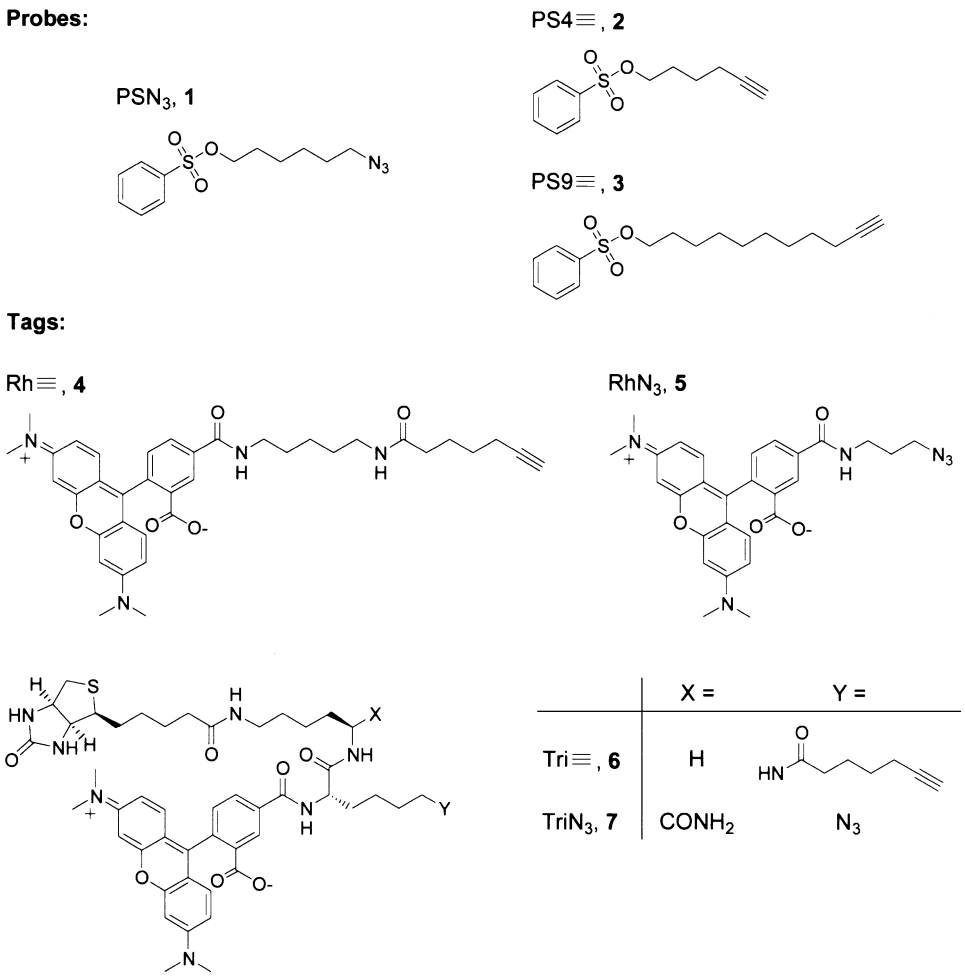

Figure 2. Chemical Structures of Azide and Alkyne Probes and Tags

Note: $TriN_3$, **7** was synthesized on solid phase and thus has an amide group in the X position where it was attached to the resin.

3A, endogenously expressed enzyme activities (e.g., enoyl-CoA hydratase 1 [ECH-1] and glutathione-S-transferase omega [GSTω]) were detected in cell/tissue proteomes using either version of CC-ABPP. Strikingly, however, a significant reduction in background labeling was observed in the PS9≡/RhN_3 CC reactions, which could largely be attributed to the inertness of the RhN_3 reporter tag, which showed negligible proteome labeling in the absence of PS9≡ (Figure 3A, lanes 6 and 12). The reduced background labeling of the PS9≡/RhN_3 reactions resulted in much improved signal to noise, enabling the visualization of lower-abundance enzyme activities, such as the heart aldehyde dehydrogenase-1 (ALDH-1; Figure 3A, lane 4), which was more difficult to detect in PSN_3/Rh≡ reactions due to nonspecific labeling of comigrating proteins (Figure 3A, lane 3).

A similar dependence on cycloaddition reaction components was observed for both the PS9≡/RhN_3 and PSN_3/Rh≡ proteome reactions (Figure 3B). For reactions of either directionality, $CuSO_4$ was necessary (lanes 5 and 10) but not sufficient (lanes 4 and 9) to promote the azide-alkyne cycloaddition. Significant signals were observed when only $CuSO_4$ and TCEP were used (lanes 3 and 8); however, the strongest fluorescent signals were achieved when ligand was also added to the reactions (lanes 1 and 6). Curiously, although protein labeling was augmented in reactions with copper and ligand compared to reactions containing only copper (e.g., lane 2 versus 4), the detection of specifically labeled enzyme activities appeared particularly dependent on the presence of reducing agent (e.g., compare labeling intensity of ECH-1 in lane 1 versus 2 or lane 6 versus 7). Regardless, in all reactions examined, the PS9≡/RhN_3 cycloaddition pair was found to exhibit significantly reduced background signals compared to PSN_3/Rh≡.

Finally, a comparison of the dependence of PS9≡/RhN_3 and PSN_3/Rh≡ reactions on tag concentration and time (Figures 3C and 3D, respectively) revealed that both cycloadditions proceeded to apparent completion by 1 hr using 50 μM tag, with the latter reaction showing approximately 4-fold faster kinetics (Figure 3D; shown for the PS target GSTω labeled in MDA-MB-435 proteomes). Collectively, these data indicate that, while CC in proteomes is likely not a simple process, it does adhere to general rules that enable the optimization of this strategy for functional proteomic investigations.

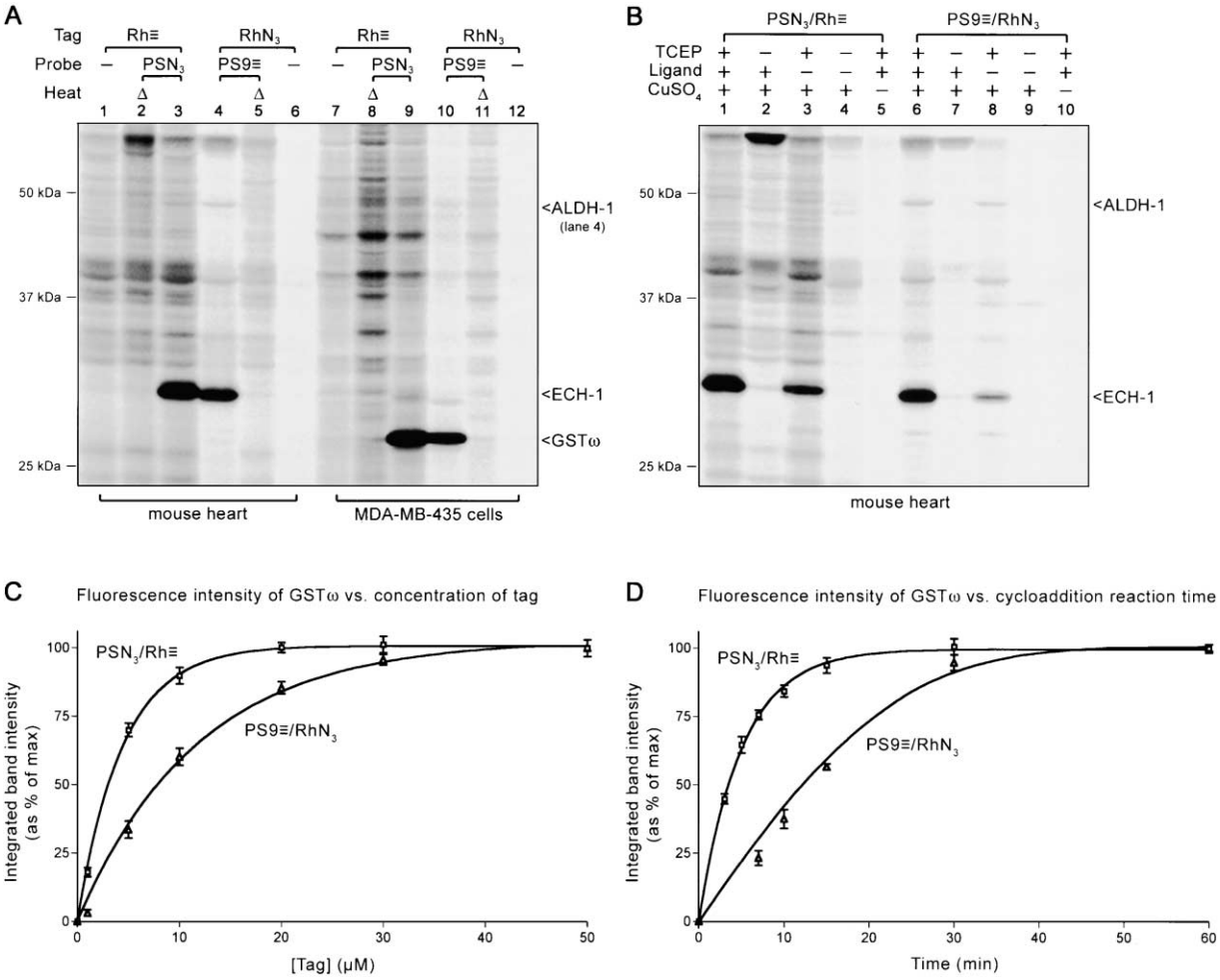

Figure 3. Comparison of In Vitro Labeling of Enzymes in Complex Proteomes Using PSN_3/Rh≡ and PS9≡/RhN_3 CC Pairs

(A) Three target enzymes, ALDH-1, ECH-1, and GSTω, are labeled by both CC pairs; Rh≡ gives rise to significant background in the presence and absence of PSN_3. Δ, heat-denatured proteomes. (B) Dependence of protein labeling on click chemistry reaction components. Strongest fluorescent signals are observed when $CuSO_4$, ligand, and TCEP are used in the cycloaddition reaction. (C and D) Fluorescence intensity of GSTω labeling (in homogenates of MDA-MB-435 cells) as a function of (C) tag concentration and (D) cycloaddition reaction time. A tag concentration of 50 μM is sufficient to achieve maximum fluorescent intensity in 1 hr (C). The PSN_3/Rh≡ CC pair reacts to completion approximately four times faster than the PS9≡/RhN_3 CC pair (D; 50 μM tag). Note: for (A) and (B) (and subsequent figures), fluorescent gel images are shown in gray scale.

Once having established optimal conditions where the CC reaction proceeded to completion in whole proteomes, we then carried out a quantitative analysis of the sensitivity limits of CC-ABPP. To estimate the minimal amount of active enzyme detectable by CC-ABPP, it was first important to select an enzyme that reacted to completion with PS probes. Indeed, although the relative levels of a given enzyme activity can be measured across proteomes by ABPP under conditions of partial probe labeling [34], estimations of the absolute quantity of active enzyme in a given proteome can only be made for fully probe-labeled enzymes [37]. Analysis of the time- and probe concentration-dependence of PSN_3/T-47D proteome reactions determined that a 1 hr treatment with 10 μM PSN_3 was sufficient to completely label the GSTω enzyme (Supplemental Figure S1 at http: / /www.chembiol.com /cgi/content/ full/ 11/4/535/ DC1). Under these conditions, comparison of the signal intensity of GSTω to signals of a serial dilution of purified fatty acid amide hydrolase labeled to completion with a rhodamine-tagged fluorophosphonate probe [37] resulted in an estimation of 0.1 pmol of GSTω per gel lane, or approximately 0.01% of the total soluble T-47D proteome (26 μg of protein loaded per lane). Notably, however, the actual sensitivity limit of CC-ABPP was at least 10-fold greater than this measurement, as GSTω could still be detected when labeled to only 10% completion. Collectively, these data highlight that CC-ABPP can quantitate the levels of active enzymes in whole proteomes with high sensitivity.

Profiling Enzyme Activities In Vivo by CC-ABPP

Previously, we reported the utilization of the PSN_3/Rh≡ CC pair for profiling enzyme activities in living cells and organisms [22]. These studies capitalized on the remarkable cellular stability of the azide group, which has also

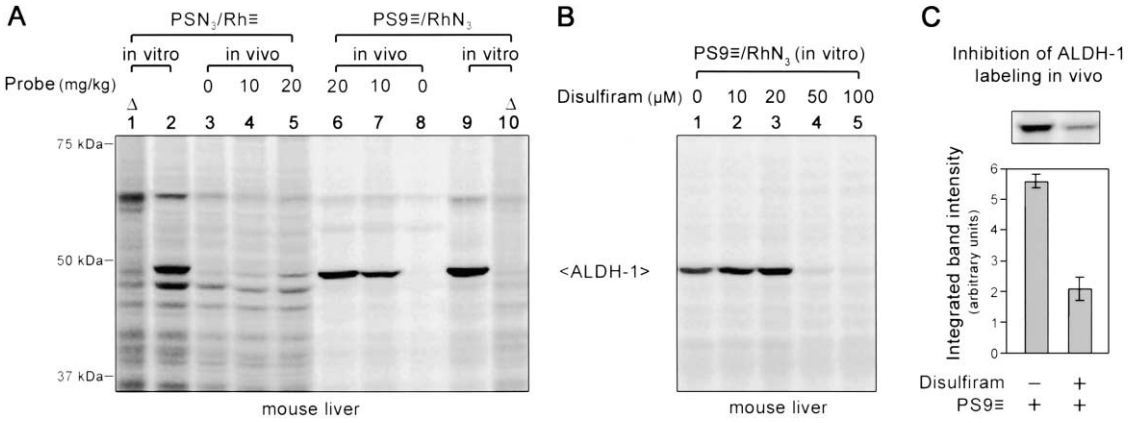

Figure 4. In Vivo Labeling of ALDH-1 in Mouse Liver

(A) Comparison of CC pairs. Clear fluorescent signals are observed for ALDH-1 when mice are treated (10, 20 mg/kg i.p.) with PS9≡ but not PSN_3. In vitro-labeled ALDH-1 shown for comparison (lanes 2 and 9) along with the associated heat controls (Δ, lanes 1 and 10).

(B) In vitro chemical inhibition of ALDH-1 by disulfiram (0–100 μM added 1 hr prior to reaction with 5 μM PS9≡).

(C) In vivo chemical inhibition of ALDH-1 by disulfiram results in a 2.6-fold reduction in labeling intensity. Representative gel image shown above the bar graph (n = 3 per group).

been exploited for incorporation of this moiety into carbohydrate and protein molecules in situ [30–33]. In contrast, fewer studies have explored the cellular stability of aliphatic alkynes [33], making it less clear whether CC-ABPP of the opposite directionality (alkyne probe/azide tag) would be applicable in vivo. To compare the ability of the PS9≡ and PSN_3 probes to detect enzyme activities in vivo, these reagents were administered to mice at doses of 10 or 20 mg/kg (intraperitoneal [i.p.]). After 1 hr, the animals were sacrificed, their liver tissue removed and homogenized, and the soluble proteome fraction subject to CC reaction conditions. In-gel fluorescence analysis of the reaction products revealed a dramatic difference in the labeling profiles of the PS9≡ and PSN_3 probes. While the primary PS-target in liver, ALDH-1, was easily visualized with PS9≡ (Figure 4A, lanes 6 and 7), the detection of this enzyme using the PSN_3 probe was obscured, at least in part, by strong background labeling (Figure 4A, lanes 4 and 5). Consistent with the in vitro studies described above, background signals in the PSN_3/Rh≡ in vivo experiments were apparently due to direct proteome labeling by the Rh≡ tag (i.e., not dependent on the presence of the PSN_3 probe; compare lane 3 to lanes 4 and 5). Finally, it is worth noting that, even after accounting for differences in background labeling, the PS9≡ probe still labeled ALDH-1 with greater efficiency than the PSN_3 probe in vivo, which contrasts with the nearly equivalent labeling of ALDH-1 by these probes in vitro. Although several factors may have accounted for the enhanced labeling of ALDH-1 by PS9≡ in vivo (e.g., superior distribution and/or uptake of this probe compared to PSN_3), these data, at a minimum, highlight that alkyne-modified probes display suitable stability for profiling enzyme activities in living animals.

Applications of CC-ABPP—The Identification of Targets of Enzyme Inhibitors In Vivo

ABPP has been applied to identify the enzyme targets of several synthetic inhibitors [13, 34] and natural products [35] directly in cell/tissue homogenates. Conceivably, CC-ABPP could enable the extension of such inhibitor profiling methods to evaluate the sites of action of enzyme inhibitors in vivo. To test this notion, a preliminary in vitro experiment was carried out with disulfiram, a known active site-directed inhibitor of ALDH-1 [36]. Treatment of soluble liver homogenate with disulfiram (50–100 μM, 1 hr) completely blocked labeling of ALDH-1 by PS9≡ (Figure 4B), confirming that CC-ABPP could detect the chemical inhibition of enzymes in whole proteomes. Next, mice were administered disulfiram (100 mg/kg i.p.) or vehicle control 1 hr prior to treatment with PS9≡ (10 mg/kg i.p.). After 1 hr, animals were sacrificed and their liver tissue processed and analyzed by CC-ABPP as described above. Disulfiram-treated mice showed a 2.6-fold reduction in ALDH-1 labeling intensity compared to vehicle-treated animals (Figure 4C). These data indicate that CC-ABPP methods can read out changes in enzyme activity in vivo due to the actions of chemical inhibitors.

Applications of CC-ABPP—The Identification of Enzyme Activities Expressed in Living Cells

One of the primary goals of ABPP is to identify enzyme activities that are differentially expressed in human disease. With this objective in mind, we recently applied ABPP to discover several novel enzyme activities upregulated in invasive human cancer cells [20, 37, 38]. In these initial studies, however, enzymes were profiled in cancer cell extracts and, therefore, certain proteins that were active only in the context of the living cell may have eluded detection. To explore this possibility, we compared the enzyme activity profiles of two human breast cancer lines using both in vitro and in situ CC-ABPP. One noninvasive, estrogen receptor (ER)-positive line, T-47D, and one invasive, ER-negative line, MDA-MB-231, were selected for analysis with the following two goals: (1) to identify enzymes activities that were differentially expressed in situ and in vitro and (2) to identify enzyme activities that were differentially ex-

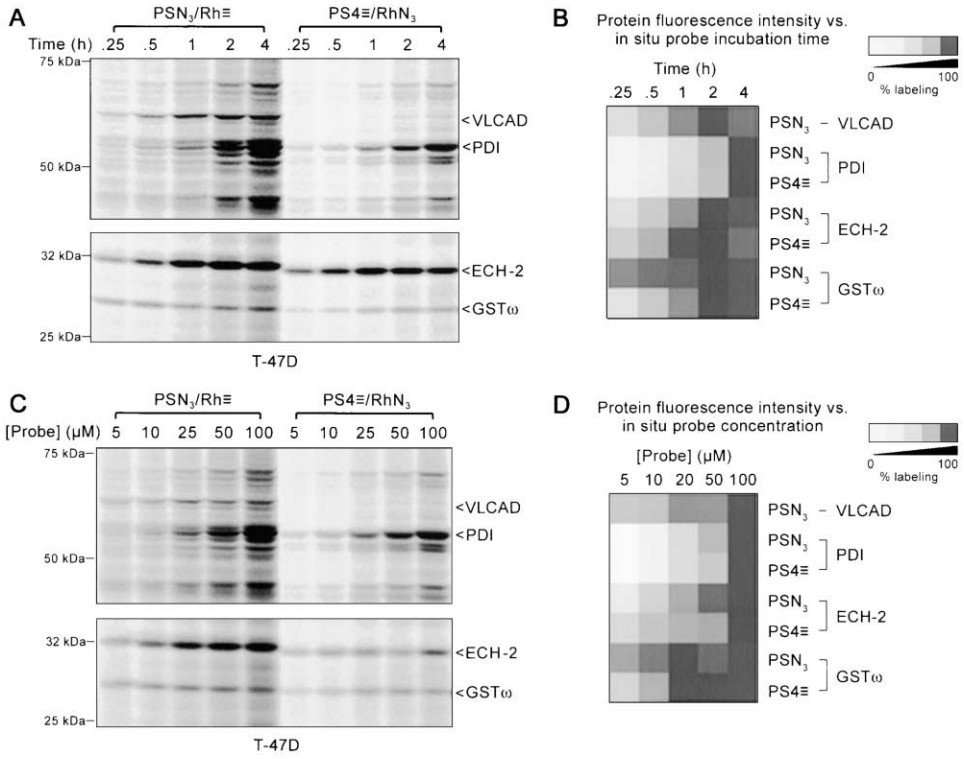

Figure 5. Time and Concentration Dependence of In Situ Probe Labeling of T-47D Cancer Cells

In situ protein labeling as a function of probe incubation time ([A] and [B], 15 min to 4 hr, 25 μM probe) and concentration ([C] and [D], 5–100 μM probe, 1 hr). Graphical representation of protein labeling intensities (each normalized to percent of maximum intensity) for time and concentration dependence gels shown in (B) and (D), respectively. For graph of absolute labeling intensities, see Supplemental Figure S2 on *Chemistry & Biology*'s website.

pressed in noninvasive (T-47D) and invasive (MDA-MB-231) breast cancer cells.

Conditions were established for the analysis of in situ enzyme activity by treating living cancer cells for variable incubation times (15 min–4 hr) with a range of concentrations of two PS probes, PSN_3 and PS4≡ (5–100 μM). Cells were then harvested and processed and the soluble proteome subject to CC reaction conditions. As is shown in Figure 5A, clear time-dependent labeling was observed for nearly all enzyme activities, confirming that these proteins were modified by probes in situ (rather than being, for example, artifactually labeled posthomogenization). A wide range of labeling kinetics was observed, with some enzyme activities reacting to completion with PS probes within 1–2 hr (e.g., GSTω, ECH-2) and other proteins exhibiting linear rates of labeling throughout the 4 hr time course (e.g., protein disulfide isomerase [PDI]) (Figure 5B). The rate of labeling of this latter group of proteins could be increased by treating cells with higher concentrations of probe (Figures 5C and 5D). Overall, the labeling profiles for the PSN_3 and PS4≡ probes were similar, with one notable exception: the enzyme very long chain acyl-CoA dehydrogenase (VLCAD), which was detected exclusively with the PSN_3 probe. Enzymes were identified utilizing trifunctional probes containing biotin and rhodamine groups (Figure 2, compounds **6** and **7**) and avidin chromatography-mass spectrometry (MS) methods, as described in the Experimental Procedures.

In situ profiles were then compared to profiles generated by in vitro ABPP to identify conditions where background signals were normalized for both methods (in situ labeling for 1 hr with 25 μM probe in 5 ml culture media; in vitro labeling for 1 hr with 5 μM probe and 2 mg/ml soluble proteome). Background signals were defined as proteins that showed heat-insensitive labeling in vitro and typically corresponded to low-level modification of abundant proteins (as judged by comparison of probe labeling profiles to Coomassie blue-stained gels; data not shown). Under normalized conditions, the enzyme activity profiles of living cancer cells were quantitatively compared to those generated in vitro (Figure 6). Several differentially expressed enzyme activities could be detected by direct analysis of proteomes by 1D-SDS-PAGE (Figure 6A); however, more complete enzyme activity profiles were generated by separation of proteomes on a Q Sepharose anion exchange column prior to 1D-SDS-PAGE analysis (Figure 7A). Two general types of enzyme activities were detected: (1) enzymes that labeled equally well in situ and in vitro (e.g., GSTω) and (2) enzymes that labeled more strongly in situ than in vitro (e.g., VLCAD, PDI, ECH-2) (Figures 6B). Notably, one enzyme activity, VLCAD, was labeled by the PSN_3 probe exclusively in living breast cancer cells, suggesting that homogenization resulted in the inactivation of this protein.

As described previously [20, 22], the PS target GSTω was found to be highly upregulated in MDA-MB-231

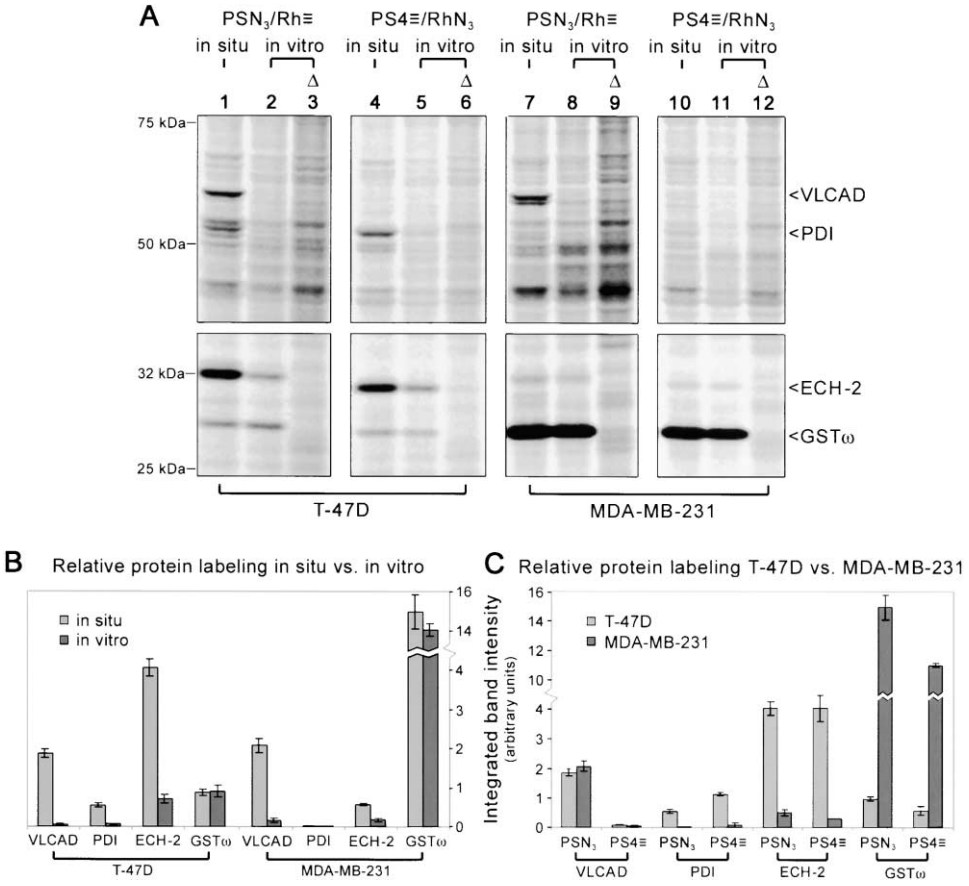

Figure 6. Comparison of In Situ and In Vitro Enzyme Activity Profiles of T-47D and MDA-MB-231 Cancer Cell Lines

(A) While some enzyme activities are labeled with equal intensity in situ and in vitro (e.g., GSTω), other enzyme activities show significantly more probe labeling in situ compared to in vitro (e.g., VLCAD). Notable differences in protein activity between the invasive (MDA-MB-231) and noninvasive (T-47D) cell lines were also observed (e.g., ECH-2). Δ, heat-denatured proteomes.

(B and C) Levels of representative enzyme activities compared (B) in situ versus in vitro (shown for PSN_3/Rh≡) and (C) in situ-labeled T-47D versus MDA-MB-231 cells (n = 3 per group).

cells as compared to T-47D cells (Figure 6C). In contrast, in situ labeling identified an enoyl-CoA hydratase (ECH) that showed higher activity in T-47D cells than MDA-MB-231 cells (Figure 6C). Interestingly, database searches revealed that this enzyme represents a previously uncharacterized ECH that shows 97% sequence identity with human ECH-1 [39]. Multiple tryptic peptides were obtained for the PS-labeled breast cancer ECH that distinguished it from ECH-1 (Figure 7B). Accordingly, we have named this novel human ECH variant ECH-2. Collectively, these results highlight that in situ profiling by CC-ABPP facilitates the identification of (1) enzymes that are labeled by activity-based probes predominantly or exclusively in living cells, (2) enzymes that are differentially expressed in invasive (MDA-MB-231) and noninvasive (T-47D) breast cancer cells, and (3) novel enzyme activities.

Discussion

Proteomic experiments are typically performed with cell/tissue samples prepared in vitro. Accordingly, these studies may fail to account for dynamic events that regulate protein function in living cells and tissues. For example, the activities of enzymes are often controlled by protein-protein interactions [2], which are sensitive to the endogenous concentrations and/or subcellular localizations of regulatory proteins. Recently, we introduced a tag-free strategy for activity-based protein profiling (ABPP) in vivo, which enables the detection of enzyme activities in their native cellular environment [22]. This tag-free version of ABPP was accomplished by engineering into activity-based probes and reporter tags an azide and alkyne group, respectively, which can react to form a stable triazole product via the Huisgen's 1,3-dipolar cycloaddition reaction (click chemistry [23]). Here, we have conducted a thorough characterization of click chemistry (CC)-ABPP and, by addressing several technical shortcomings and challenges, identified optimal conditions for profiling enzyme activities in living cells and organisms by this method.

The first experimental challenge addressed in this study was the inferior sensitivity of CC-ABPP compared to standard ABPP. In our original description of CC-ABPP, proteomes were treated with an azide-modified phenyl sulfonate ester probe (PSN_3) and protein-labeling events

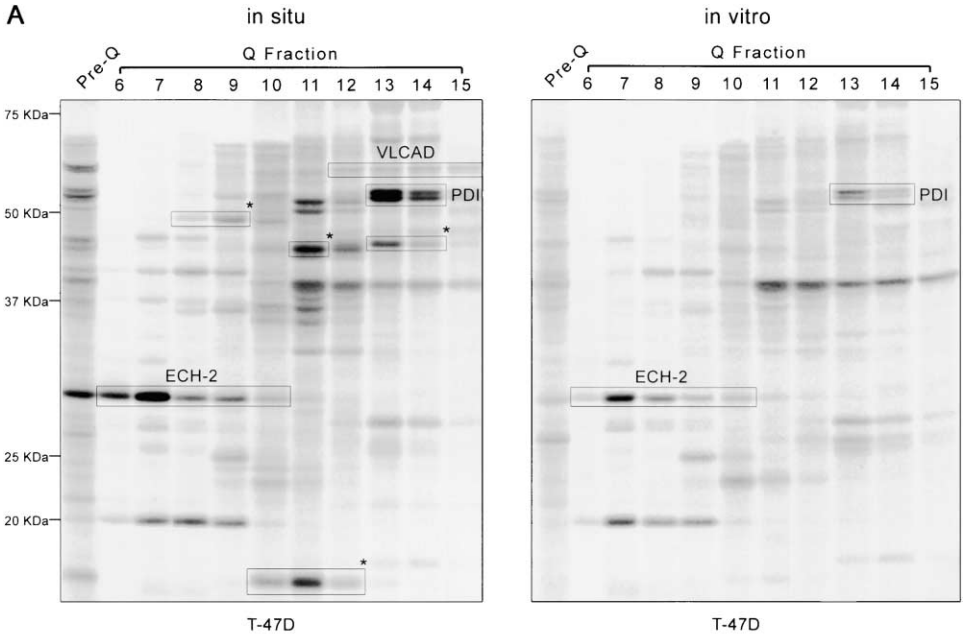

B

Data from nanoLC-MS/MS for ECH-2

Peptides common to both ECH-1 and -2	Peptides unique to ECH-2	
319-ELK-321	232-MMADEALGSGLVSR-245	ECH-2
138-ISWYLR-143	232-MMADEALDSGLVSR-245	ECH-1
277-VNLLYSR-283		
1-MAAGIVASRR-10	231-KMMADEALGSGLVSR-245	ECH-2
88-EMVECFNK-95	231-KMMADEALDSGLVSR-245	ECH-1
149-YQETFNVIER-158		
186-YCAQDAFFQVK-196	215-VIGNQSLVNELAFTAR-230	ECH-2
197-EVDVGLAADVGTLQ/ER-211	215-VIGNQSLVNELAFTAL-230	ECH-1
113-MFTAGIDLMDMASDILQPK-131		

Figure 7. Q-Sepharose Chromatography of In Situ and In Vitro Probe-Labeled T-47D Proteomes Enhances the Visualization of Differentially Expressed Enzyme Activities

(A) Several proteins that exhibited stronger or exclusive labeling in situ are boxed, including enzyme activities that could be detected by 1D-SDS-PAGE analysis of whole proteomes (e.g., ECH-2, PDI, VLCAD; see Figure 6A) and other proteins that were more effectively visualized following Q fractionation (asterisks).

(B) MS peptide data (black text) for a novel human enoyl-CoA hydratase variant, ECH-2. Residues that distinguish ECH-2 from the previously identified ECH-1 [39] are boxed.

were visualized upon reaction with an alkyne-derivatized rhodamine tag (Rh≡) [22]. Although this version of CC-ABPP detected enzyme activities in whole proteomes with signal intensities comparable to standard ABPP methods, it also suffered from significantly higher background labeling both in vitro and in vivo. Here, we determined that the background labeling of PSN_3/Rh≡ reactions was not dependent on the presence of the azide probe and thus could be attributed to the reactivity of the alkyne reporter tag. This nonspecific modification of proteins by Rh≡ was only observed in the presence of copper and was further exacerbated by ligand and TCEP. In contrast, no background proteome labeling was detected with an azide-modified Rh tag (RhN_3) either in vitro or in vivo. As a consequence, CC-ABPP reactions conducted with a PS≡ probe and RhN_3 tag showed significantly improved signal to noise and sensitivity, facilitating the visualization of low-abundance enzyme activities that eluded detection in PSN_3/Rh≡ reactions. Still, a comparison of the kinetics of each version of CC-ABPP revealed that PSN_3/Rh≡ reactions were faster, reaching completion in approximately one-fourth the time of PS≡/RhN_3 reactions. Thus, each version of CC-ABPP possesses distinct advantages: the PSN_3/Rh≡ pair may be more applicable when rapid sample analysis is desired, while the PS≡/RhN_3 combination should be more suitable for investigations requiring the highest level of sensitivity.

Having observed superior sensitivity with the PS≡/RhN_3 pair, we next asked whether this version of CC-ABPP could be applied in vivo. Indeed, while azides are known to exhibit exceptional cellular stability and have been exploited by several groups for the in situ modification of biomolecules [30–33], less is understood about the suitability of alkynes as components of cellular probes. For example, alkynes could be prone to enzymatic reduction in vivo, especially in metabolically active tissues like the liver [40]. However, we found that alkyne-modified phenyl sulfonate ester probes served as excellent profiling agents both in living cells and organisms,

permitting, for example, the in vivo detection of the liver enzyme activity aldehyde dehydrogenase-1 with a signal intensity and sensitivity that surpassed that of the PSN_3 probe. Thus, these findings suggest that either azide- or alkyne-modified activity-based probes can be utilized to profile enzyme activities in vivo.

To date, standard ABPP methods have been applied to several biological systems, enabling the discovery of both disease-associated enzyme activities and specific inhibitors of these enzymes using cell/tissue homogenates [21]. Here, we have demonstrated that similar biological applications can be pursued in vivo using CC-ABPP. For example, the inhibition of ALDH-1 in vivo by the active site-directed agent disulfiram could be quantified by CC-ABPP, indicating that this method may be used to confirm whether and to what extent drugs inhibit their intended (as well as potentially unintended) targets in animal models. Given the myriad issues that may affect the efficacy of inhibitors in animals, including uptake, distribution, and metabolism, the value of new technologies that can assess inhibitor activity in vivo is evident. In this regard, however, it should be noted that disulfiram is a covalent inhibitor of ALDH-1 and therefore simpler to evaluate by ABPP than reversible inhibitors, for which more complex kinetic factors must be taken into account. Still, standard ABPP has recently been adapted for the analysis of reversible enzyme inhibitors in cell/tissue homogenates [34], and, following a similar approach, we anticipate that CC-ABPP can be optimized for the characterization of the activity of reversible inhibitors in vivo.

We also applied CC-ABPP to compare the in situ versus in vitro enzyme activity profiles of human breast cancer cell lines, resulting in the identification of enzymes that were labeled by PS probes predominantly or exclusively in living cells but not in cell homogenates. These enzymes included a novel enoyl-CoA hydratase variant ECH-2 that was upregulated in noninvasive breast cancer cells; PDI, a multifunction enzyme that catalyzes the formation and isomerization of disulfide bonds in addition to functioning as a molecular chaperone and subunit of prolyl 4-hydroxylase and microsomal triglyceride transfer protein [41–43]; and VLCAD, a mitochondrial flavoprotein that catalyzes the β oxidation of very long chain acyl-CoA esters [44, 45]. Interestingly, previous studies have shown that VLCAD, as well as other acyl-CoA dehydrogenases, are rapidly inactivated by binding to CoA persulfide in cell and/or tissue preparations [45]. This event, also referred to as "greening" because it results in dehydrogenases appearing green in color, has been suggested to reflect a mode by which these enzymes may be regulated posttranslationally in vivo [45]. Thus, the selective labeling of VLCAD in living breast cancer cells may reflect the inactivation of this enzyme by CoA persulfide upon homogenization. More generally, these findings highlight the value of performing ABPP experiments in living cells, especially for enzyme activities that are sensitive to posttranslational forms of regulation.

Several challenges still face the application of CC-ABPP and related methods for profiling enzyme function in vivo, especially as pertains to data analysis and interpretation. For example, distinguishing specific from nonspecific protein labeling events is more challenging for in vivo ABPP studies, which lack the straightforward controls devised for in vitro ABPP (e.g., comparative profiling of native and heat-denatured proteomes). Accordingly, confirmation that probe-enzyme reactions observed in vivo actually occur in enzyme active sites (i.e., in an "activity-based" manner) may require the identification of sites of probe modification. Fortunately, a gel-free version of ABPP has recently been introduced to identify specific sites of probe labeling on enzymes isolated from whole proteomes [46]. Thus, a combination of gel-based and gel-free methods for CC-ABPP should enable both the identification and thorough characterization of probe-enzyme reactions that occur in vivo. When applying ABPP in vivo, one must also confront the problem of interpreting the biological significance of probe-enzyme reactions that occur in living cells/organisms but not in vitro. Although the most obvious (and perhaps enticing) interpretation of such data is that they reflect enzyme activities that are tightly regulated by posttranslational mechanisms (e.g., CoA persulfide inactivation of VLCAD), other explanations are also possible. For example, if certain activity-based probes distribute into specific cellular compartments (rather than equally throughout the cell), then enzyme activities localized to these structures may show disproportionately enhanced labeling in vivo. In the end, sorting through the intriguing biological implications afforded by in vivo activity-based profiling will likely require detailed biochemical and cell biological investigations. Regardless, it is clear from the studies described herein that CC-ABPP offers a valuable complement to standard ABPP methods, especially for the identification and characterization of enzymes that are regulated by posttranslational mechanisms in vivo.

Significance

The field of proteomics aims to develop and apply methods for the global analysis of protein expression and function. Toward this end, strategies for profiling protein activity in vivo would be particularly valuable. Here, we describe the detailed characterization of a tag-free version of activity-based protein profiling (ABPP) that utilizes the azide-alkyne cycloaddition reaction (click chemistry) to analyze the functional state of enzymes in living cells and animals. We establish conditions that maximize the speed, sensitivity, and bioorthogonality of click chemistry-ABPP and apply this strategy to identify enzymes that are labeled by activity-based probes in vivo but not in vitro. Notably, some of these enzyme activities were differentially expressed in invasive and noninvasive breast cancer cells, suggesting that they may represent novel markers and/or targets for this disease. Additionally, click chemistry-ABPP was used to measure changes in enzyme activity in mice due to the action of chemical inhibitors, indicating that this method may be implemented to test whether drugs inhibit their intended targets in vivo. Collectively, these studies highlight the value of click chemistry-ABPP and related functional proteomic methods that can evaluate the activity of proteins in living cells and organisms.

Experimental Procedures

Synthesis of Probes and Tags

See Supplemental Data on *Chemistry & Biology*'s website.

Proteome Sample Preparation, Probe Labeling, Cycloaddition, and Protein Detection

Preparation of Mouse Tissue Soluble Proteomes

Mouse tissues were Dounce homogenized in 10 mM sodium/potassium phosphate buffer (pH 8.0) (PB), and the soluble fraction was isolated using high-speed centrifugation to remove the heavy and light membrane components: 22,000 × *g* (30 min, pellet = heavy membrane fraction) and 100,000 × *g* (60 min, pellet = light membrane, supernatant = soluble fraction). Prepared soluble proteome samples were diluted to 2.0 mg/ml in PB and stored at −80°C until use.

Preparation of Cell Line Soluble Proteomes

Cell lines were grown to 80% confluency in RPMI-1640 medium (Invitrogen) containing 10% fetal calf serum (FCS). Cells were harvested, sonicated, Dounce homogenized in PB, and centrifuged at 100,000 × *g* (45 min) to isolate the soluble fraction (supernatant). Prepared samples were diluted to 2.0 mg/ml in PB and stored at −80°C until use.

In Vitro Labeling of Proteins

Proteome samples (43 μl of 2.0 mg/ml protein in PB) were treated with 5 μM (unless otherwise indicated) PS probe (44× stock in dimethyl sulfoxide [DMSO]) for 1 hr at room temperature (43 μl reactions were set up so that, once the cycloaddition reagents were added, the total reaction volume would be 50 μl). For heated controls, proteome samples were heated at 80°C for 5 min prior to addition of PS probe. To facilitate higher throughput, probe reactions (and cycloadditions) were carried out in PCR tubes (strips of 12 × 200 μl) using multichannel multipipettors to dispense reagents.

In Vivo Labeling of ALDH-1 in Mice

Mice were given intraperitoneal (i.p.) injections of 10 or 20 mg/kg PS probe (in vehicle [18:1:1 saline:emulphor:EtOH]). (Mock injected mice received i.p. injection of vehicle alone.) After 1 hr, the mice were anesthetized in O_2/CO_2 mixture, sacrificed by decapitation, and liver tissue was collected, frozen in dry ice (30 min), and processed as described to isolate the soluble proteome. For inhibition experiment with disulfiram, mice were given i.p. injections of 100 mg/kg disulfuram (in vehicle [18:1:1 saline:emulphor:DMSO]) 1 hr prior to administration of PS9≡ (10 mg/kg, 1 hr) and treated as described above to isolate soluble liver proteome. (Mice used for nondisulfiram comparison received injection of vehicle alone.)

In Situ Labeling of Proteins in Cancer Cell Lines

Cell lines were grown to 80% confluency in RPMI-1640 medium (Invitrogen) containing 10% FCS. Prior to in situ labeling, cell cultures were washed (2 × 5 ml Dulbecco's phosphate buffered saline [PBS], Invitrogen) and fresh medium (5 ml RPMI-1640 containing 10% FCS) was added. Cell cultures were treated with 25 μM (unless otherwise indicated) PS probe (1000× stock in DMSO) for 1 hr (unless otherwise indicated), then washed (2 × 5 ml Dulbecco's PBS) and processed as described to isolate soluble proteome.

Cycloaddition Reactions, Protein Electrophoresis, and In-Gel Fluorescence Scanning

Following incubation with the PS probe (see above), 50–100 μM of the appropriate tag (50× stock in DMSO) was added to each protein sample (44 μl in PB), followed by 1 mM TCEP (50× stock in water) and 100 μM ligand (17× stock in DMSO:t-butanol 1:4), giving a t-butanol concentration of 5%. Samples were gently vortexed and 1 mM $CuSO_4$ (50× stock in water) was added to each proteome sample, making the total reaction volume 50 μl. Samples were vortexed again and allowed to react at room temperature for 1 hr (unless otherwise indicated), at which time 50 μl (1 volume) of standard 2×SDS-PAGE loading buffer (reducing) was added to each reaction. Note that this optimized protocol differs from that previously reported in several aspects: the reactions were not run under an inert atmosphere, no effort was made to exclude DMSO, a lower concentration of ligand was used (100 μM versus 2 mM), and excess reagents were not removed prior to electrophoresis. As mentioned above, reactions were also carried out in PCR tubes using multichannel multipipettors to facilitate higher throughput. For time course experiments with GSTω, reactions were quenched with loading buffer containing either 10 mM 5-hexyn-1-ol (for PSN_3/Rh≡) or 10 mM 6-azido hexan-1-ol (for PS9≡/RhN_3) to block any further cycloaddition between probe-labeled enzymes and the azide/alkyne tags. Proteins were separated by 1D SDS-PAGE (26 μg of protein/gel lane) and visualized in-gel using a Hitachi FMBio IIe flatbed laser-induced fluorescence scanner (MiraiBio, Alameda, CA). Labeled proteins were quantified by measuring integrated band intensities (normalized for volume). For all quantification experiments, n = 3 trials per data point and error represents ±standard deviation of the average of these values.

Protein Isolation and Identification from Cancer Cell Lines

In standard ABPP, biotinylated and/or trifunctional probes (bearing both biotin and rhodamine functional groups) are utilized to affinity purify enzyme activities, enabling their identification by mass spectrometry techniques [38]. Similarly, for CC-ABPP, trifunctional azides or alkynes were employed as reporter tags. Large-scale cell cultures (3 to 4 × 150 mm plates, each containing 10 ml medium) were treated with PS probe for 2 to 4 hr (depending on labeling kinetics of target protein), after which point cells were washed, homogenized, and centrifuged to isolate the soluble fraction as described above. The soluble proteome (2.5 ml at 2 to 3 mg/ml) was applied to a PD-10 size exclusion column and eluted with 3.5 ml PB. Proteomic samples were then fractionated by Q-Sepharose chromatography (0–2 M NaCl gradient). Diagnostic cycloaddition reactions (20 μl of each 500 μl fraction) were then run to identify fractions containing desired protein(s), which were then reacted with the appropriate trifunctional probe (20 μM; 180 μl reactions). After 1 hr, cold PB (200 μl) was added, and the reactions were centrifuged (5900 × *g*, 4 min, 4°C) to pellet the protein. The supernatant containing excess cycloaddition reagents was removed, and cold methanol (200 μl) was added to the protein pellet, which was resuspended by sonication (3–5 s) and allowed to rotate at 4°C for 10 min. The sample was then centrifuged (5900 × *g*, 4 min, 4°C) and the supernatant removed. Following a second methanol wash, proteins were solubilized in PB containing 0.5% SDS via sonication (3–5 s) and affinity-isolated using avidin-agarose beads (Sigma) as described previously [11, 19]. Affinity-isolated proteins were separated/visualized by SDS-PAGE and in-gel fluorescence scanning. Previously, Coomassie staining was used to directly visualize the protein band, which was then removed for mass spectrometry (MS) analysis. However, even after enrichment, probe-labeled proteins were often difficult to see by Coomassie staining, and distortion of the gel during the stain/destain process made comparison with the fluorescent image/Western blot difficult. We found that it was effective to cut the protein bands out of the unstained gel using a corresponding fluorescent gel image as a template. After the initial fluorescent scan, sections above and below the band of interest were carefully excised, the gel rescanned, and the cut refined. After two to three iterations, the band was sufficiently localized that it could be cleanly removed. In addition to shortening the protein isolation protocol, the stain-free procedure increased certainty of cutting the right band and it alleviated the need to use staining reagents that could complicate protein identification. Isolated gel slices were washed with methanol:water:acetic acid (5:4:1) for 1 hr, then methanol:water (1:1; 1 hr, then 12 hr with fresh solution) and subject to in-gel trypsin digest. The resulting peptides were analyzed by nanoLC-MS/MS and results searched against public databases to identify probe-labeled proteins. VLCAD (gi:18044943) was independently identified from both T-47D and MDA-MB-231 cells, and ECH-2 (gi:15080016) and PDI (gi: 20070125) were identified from T-47D cells.

Supplemental Data

The Supplemental Data available at http://www.chembiol.com/cgi/content/full/11/4/535/DC1 includes synthesis of probes and tags and graphs of in vitro (GSTω) and in situ enzyme labeling in T-47D proteome.

Acknowledgments

We thank the Finn, Sharpless, and Cravatt labs for helpful discussions; Dr. Greg Adam for contributions to the project; and G. Hawkins and M. Humphrey for technical assistance. This work was supported by the National Institutes of Health (Grant no. CA87660), the California Breast Cancer Research Program, The Skaggs Institute for Chemical Biology, and a Howard Hughes Medical Institute predoctoral fellowship (to A.E.S.).

Received: December 8, 2003
Revised: January 19, 2004
Accepted: January 21, 2004
Published: April 16, 2004

References

1. Kodadek, T. (2001). Protein microarrays: prospects and problems. Chem. Biol. *8*, 105–115.
2. Kobe, B., and Kemp, B.E. (1999). Active site-directed protein regulation. Nature *402*, 373–376.
3. Corthals, G.L., Wasinger, V.C., Hochstrasser, D.F., and Sanchesz, J.C. (2000). The dynamic range of protein expression: a challenge for proteomic research. Electrophoresis *21*, 1104–1115.
4. Santoni, V., Molloy, M., and Rabilloud, T. (2000). Membrane proteins and proteomics: un amour impossible? Electrophoresis *21*, 1054–1070.
5. Harry, J.L., Wilkins, M.R., Herbert, B.R., Packer, N.H., Gooley, A.A., and Williams, K.L. (2000). Proteomics: capacity versus utility. Electrophoresis *21*, 1071–1081.
6. Gygi, S.P., Corthals, G.L., Zhang, Y., Rochon, Y., and Aebersold, R. (2000). Evaluation of two-dimensional gel electrophoresis-based proteome analysis technology. Proc. Natl. Acad. Sci. USA *97*, 9390–9395.
7. Gygi, S.P., Rist, B., Gerber, S.A., Turecek, F., Gelb, M.H., and Aebersold, R. (1999). Quantitative analysis of complex protein mixtures using isotope-coded affinity tags. Nat. Biotechnol. *17*, 994–999.
8. Han, D.K., Eng, J., Zhou, H., and Aebersold, R. (2001). Quantitative profiling of differentiation-induced microsomal proteins using isotope-coded affinity tags and mass spectrometry. Nat. Biotechnol. *19*, 946–951.
9. Cravatt, B.F., and Sorensen, E.J. (2000). Chemical strategies for the global analysis of protein function. Curr. Opin. Chem. Biol. *4*, 663–668.
10. Adam, G.C., Sorensen, E.J., and Cravatt, B.F. (2002). Chemical strategies for functional proteomics. Mol. Cell. Proteomics *1*, 781–790.
11. Kidd, D., Liu, Y., and Cravatt, B.F. (2001). Profiling serine hydrolase activities in complex proteomes. Biochemistry *40*, 4005–4015.
12. Liu, Y., Patricelli, M.P., and Cravatt, B.F. (1999). Activity-based protein profiling: the serine hydrolases. Proc. Natl. Acad. Sci. USA *96*, 14694–14699.
13. Greenbaum, D., Baruch, A., Hayrapetian, L., Darula, Z., Burlingame, A., Medzihradszky, K.F., and Bogyo, M. (2002). Chemical approaches for functionally probing the proteome. Mol. Cell. Proteomics *1*, 60–68.
14. Thornberry, N.A., Peterson, E.P., Zhao, J.J., Howard, A.D., Griffin, P.R., and Chapman, K.T. (1994). Inactivation of interleukin-1 beta converting enzyme by peptide (acyloxy)methyl ketones. Biochemistry *33*, 3934–3940.
15. Faleiro, L., Kobayashi, R., Fearnhead, H., and Lazebnik, Y. (1997). Multiple species of CPP32 and Mch2 are the major active caspases present in apoptotic cells. EMBO J. *16*, 2271–2281.
16. Martins, L.M., Kottke, T., Mesner, P.W., Basi, G.S., Sinha, S., Frigon, N., Jr., Tatar, E., Tung, J.S., Bryant, K., Takahashi, A., et al. (1997). Activation of multiple interleukin-1beta converting enzyme homologues in cytosol and nuclei of HL-60 cells during etoposide-induced apoptosis. J. Biol. Chem. *272*, 7421–7430.
17. Lo, L.C., Pang, T.L., Kuo, C.H., Chiang, Y.L., Wang, H.Y., and Lin, J.J. (2002). Design and synthesis of class-selective activity probes for protein tyrosine phosphatases. J. Proteome Res. *1*, 35–40.
18. Tsai, C.S., Li, Y.K., and Lo, L.C. (2002). Design and synthesis of activity probes for glycosidases. Org. Lett. *4*, 3607–3610.
19. Adam, G.C., Cravatt, B.F., and Sorensen, E.J. (2001). Profiling the specific reactivity of the proteome with non-directed activity-based probes. Chem. Biol. *8*, 81–95.
20. Adam, G.C., Sorensen, E.J., and Cravatt, B.F. (2002). Proteomic profiling of mechanistically distinct enzyme classes using a common chemotype. Nat. Biotechnol. *20*, 805–809.
21. Speers, A.E., and Cravatt, B.F. (2004). Chemical strategies for activity-based proteomics. Chembiochem *5*, 41–47.
22. Speers, A.E., Adam, G.C., and Cravatt, B.F. (2003). Activity-based protein profiling in vivo using a copper(I)-catalyzed azide-alkyne [3 + 2] cycloaddition. J. Am. Chem. Soc. *125*, 4686–4687.
23. Kolb, H.C., Finn, M.G., and Sharpless, K.B. (2001). Click chemistry: diverse chemical function from a few good reactions. Angew. Chem. Int. Ed. Engl. *40*, 2004–2021.
24. Lewis, W.G., Green, L.G., Grynszpan, F., Radic, Z., Carlier, P.R., Taylor, P., Finn, M.G., and Sharpless, K.B. (2002). Click chemistry in situ: acetylcholinesterase as a reaction vessel for the selective assembly of a femtomolar inhibitor from an array of building blocks. Angew. Chem. Int. Ed. Engl. *41*, 1053–1057.
25. Rostovtsev, V.V., Green, L.G., Fokin, V.V., and Sharpless, K.B. (2002). A stepwise Huisgen cycloaddition process: copper(I)-catalyzed regioselective "ligation" of azides and terminal alkynes. Angew. Chem. Int. Ed. Engl. *41*, 2596–2599.
26. Tornoe, C.W., Christensen, C., and Meldal, M. (2002). Peptidotriazoles on solid phase: [1,2,3]-triazoles by regiospecific copper(I)-catalyzed 1,3-dipolar cycloadditions of terminal alkynes to azides. J. Org. Chem. *67*, 3057–3064.
27. Wang, Q., Chan, T.R., Hilgraf, R., Fokin, V.V., Sharpless, K.B., and Finn, M.G. (2003). Bioconjugation by copper(I)-catalyzed azide-alkyne [3 + 2] cycloaddition. J. Am. Chem. Soc. *125*, 3192–3193.
28. Breinbauer, R., and Köhn, M. (2003). Azide-alkyne coupling: a powerful reaction for bioconjugate chemistry. Chembiochem *4*, 1147–1149.
29. Ovaa, H., Van Swieten, P.F., Kessler, B.M., Leeuwenburgh, M.A., Fiebiger, E., Van Den Nieuwendijk, A.M., Galardy, P.J., Van Der Marel, G.A., Ploegh, H.L., and Overkleeft, H.S. (2003). Chemistry in living cells: detection of active proteasomes by a two-step labeling strategy. Angew. Chem. Int. Ed. Engl. *42*, 3626–3629.
30. Kiick, K.L., Saxon, E., Tirrell, D.A., and Bertozzi, C.R. (2002). Incorporation of azides into recombinant proteins for chemoselective modification by the Staudinger ligation. Proc. Natl. Acad. Sci. USA *99*, 19–24.
31. Luchansky, S.J., Hang, H.C., Saxon, E., Grunwell, J.R., Yu, C., Dube, D.H., and Bertozzi, C.R. (2003). Constructing azide-labeled cell surfaces using polysaccharide biosynthetic pathways. Methods Enzymol. *362*, 249–272.
32. Link, A.J., and Tirrell, D.A. (2003). Cell surface labeling of Escherichia coli via copper(I)-catalyzed [3 + 2] cycloaddition. J. Am. Chem. Soc. *125*, 11164–11165.
33. Deiters, A., Cropp, T.A., Mukherji, M., Chin, J.W., Anderson, J.C., and Schultz, P.G. (2003). Adding amino acids with novel reactivity to the genetic code of Saccharomyces cerevisiae. J. Am. Chem. Soc. *125*, 11782–11783.
34. Leung, D., Hardouin, C., Boger, D.L., and Cravatt, B.F. (2003). Discovering potent and selective reversible inhibitors of enzymes in complex proteomes. Nat. Biotechnol. *21*, 687–691.
35. Adam, G.C., Vanderwal, C.D., Sorensen, E.J., and Cravatt, B.F. (2003). (−)-FR182877 is a potent and selective inhibitor of carboxylesterase-1. Angew. Chem. Int. Ed. Engl. *42*, 5480–5484.
36. Lipsky, J.J., Shen, M.L., and Naylor, S. (2001). In vivo inhibition of aldehyde dehydrogenase by disulfiram. Chem. Biol. Interact. *130–132*, 93–102.
37. Jessani, N., Liu, Y., Humphrey, M., and Cravatt, B.F. (2002). Enzyme activity profiles of the secreted and membrane proteome that depict cancer cell invasiveness. Proc. Natl. Acad. Sci. USA *99*, 10335–10340.
38. Adam, G.C., Sorensen, E.J., and Cravatt, B.F. (2002). Trifunctional chemical probes for the consolidated detection and iden-

tification of enzyme activities from complex proteomes. Mol. Cell. Proteomics *1*, 828–835.

39. FitzPatrick, D.R., Germain-Lee, E., and Valle, D. (1995). Isolation and characterization of rat and human cDNAs encoding a novel putative peroxisomal enoyl-CoA hydratase. Genomics *27*, 457–466.
40. Kitamura, S., Kohno, Y., Okamoto, Y., Takeshita, M., and Ohta, S. (2002). Reductive metabolism of an alpha,beta-ketoalkyne, 4-phenyl-3-butyn-2-one, by rat liver preparations. Drug Metab. Dispos. *30*, 414–420.
41. Schwaller, M., Wilkinson, B., and Gilbert, H.F. (2003). Reduction-reoxidation cycles contribute to catalysis of disulfide isomerization by protein-disulfide isomerase. J. Biol. Chem. *278*, 7154–7159.
42. Wang, C.C. (2002). Protein disulfide isomerase as an enzyme and a chaperone in protein folding. Methods Enzymol. *348*, 66–75.
43. Ruoppolo, M., Orru, S., Talamo, F., Ljung, J., Pirneskoski, A., Kivirikko, K.I., Marino, G., and Koivunen, P. (2003). Mutations in domain a′ of protein disulfide isomerase affect the folding pathway of bovine pancreatic ribonuclease A. Protein Sci. *12*, 939–952.
44. Souri, M., Aoyama, T., Cox, G.F., and Hashimoto, T. (1998). Catalytic and FAD-binding residues of mitochondrial very long chain acyl-coenzyme A dehydrogenase. J. Biol. Chem. *273*, 4227–4231.
45. Williamson, G., Engel, P.C., Mizzer, J.P., Thorpe, C., and Massey, V. (1982). Evidence that the greening ligand in native butyryl-CoA dehydrogenase is a CoA persulfide. J. Biol. Chem. *257*, 4314–4320.
46. Adam, G.C., Burbaum, J.J., Kozarich, J.W., Patricelli, M.P., and Cravatt, B.F. (2004). Mapping enzyme active sites in complex proteomes. J. Am. Chem. Soc. *126*, 1363–1368.